Energy Consumption of Geared DC Motors in Dynamic Applications: Comparing Modeling Approaches

Verstraten, Tom; Furnemont, Raphaël; Mathijssen, Glenn; Vanderborght, Bram; Lefeber, Dirk

Published in:
IEEE Robotics and Automation Letters

DOI:
10.1109/LRA.2016.2517820

Publication date:
2016

Document Version:
Accepted author manuscript

Energy Consumption of Geared DC Motors in Dynamic Applications: Comparing Modeling Approaches

Tom Verstraten, Raphael Furnémont, Glenn Mathijssen, Bram Vanderborght and Dirk Lefeber

***Abstract*—In recent years, many works have appeared which present novel mechanical designs, control strategies or trajectory planning algorithms for improved energy efficiency. The actuator model is an essential part of these works, since the optimization of energy consumption strongly depends of the accuracy of this model. Nevertheless, various authors follow very different approaches, often neglecting speed- and load-dependent losses and inertias of components such as the motor and the gearbox. Furthermore, there is no consensus on how negative power affects power consumption. Some authors calculate energy consumption by integrating the electrical power entirely, by integrating its absolute value, or by integrating only positive power. This paper assesses how well commonly used models succeed in predicting the energy consumption of an 80 W geared DC motor performing a dynamic task, by comparing the results they produce to experimental baseline measurements.**

***Index Terms*—Energy and Environment-aware Automation; Optimization and Optimal Control; Simulation and Animation**

I. Introduction

MANY fields in robotics investigate mobile applications such as prosthetics, exoskeletons, robots for exploration etc. One of the concerns in these fields is the autonomy of the power supply, typically battery packs. Although battery capacity has increased over the past years, batteries still take up a huge part of the total weight and size of such systems. An elegant way of solving this problem is to reduce the energy consumption of the actuators. Many authors have attempted to achieve this through modifications in trajectory planning, control or mechanical design - typically by adding compliant elements to the typical gearbox-motor combination. A representative model is an important condition to obtain optimal solutions or to be able to compare different designs. Still, recent publications adopt very different methods when it comes to the calculation of energy consumption. Many authors base their calculations entirely on mechanical energy consumption at the output shaft of the gearbox [1][2][3][4][5][6][7], not taking into account the efficiency of the gearbox and the motor. As most efficiencies are load- and speed-dependent, something which is especially the case for DC motors, one can expect that the most efficient solution in terms of mechanical energy consumption will not necessarily be the best solution in terms of electrical energy consumption. In this regard, interesting results were presented in [8], in which an optimization is performed on a robotic arm. Here, the authors claim having achieved two third of their energy savings due to a more efficient use of the DC motor. For this reason, some authors have implemented a DC motor model in order to improve their calculations. It often only contains a term representing the losses due to the resistance of the motor windings [9][10][11], but sometimes also a damping or friction term to match the model with the no-load current [8][12][13]. In most cases, motor inertia is included into the model, although the inertia of the gearbox is mostly neglected, a rare exception being [11]. This can have important consequences for the accuracy of dynamic models, since in many actuator systems the reflected inertia of the motor and gearbox is much larger than the inertia of the link itself [14].

The calculation of energy consumption from the consumed power is another issue on which papers disagree. Integrating the absolute value of power (or, in optimizations, its square) is very common, especially in the fields of prosthetics and exoskeletons [1][2][4][5][15][16]. There are, however, many authors who directly use the power as integrand, without taking the absolute value [3][8][10][17]. In some cases, the authors discard any negative power, only integrating over the regions of positive power [18][19].

The aim of this paper is to assess the quality of different models of varying complexity by using them to calculate the energy consumption for a simple task - an 80W geared DC motor applying a sinusoidal trajectory to a pendulum - and comparing those results to experiments. In Section II, we present four models commonly found in literature, and we give some background about the calculation of energy from power. Section III introduces the setup that was used to provide the baseline measurement, as well as the trajectories that will be imposed to the load and the torques that result from them. A comparison of the models, based on the power profiles and energy consumptions they yield, is presented in Section IV. Finally, we will discuss to what extent the models are suited to predict the energy consumption of a geared DC motor, depending on the load and trajectory (Section V).

Manuscript received: July 31, 2015; Revised October 28, 2015; Accepted December 22, 2015.

This paper was recommended for publication by Editor Antonio Bicchi upon evaluation of the Associate Editor and Reviewers' comments. The first and third author have a personal grant from the Research Foundation Flanders - Fonds voor Wetenschappelijk Onderzoek (FWO). Part of this work was funded by the European Commission ERC Starting grant SPEAR (no. 337596).

All authors are with the Robotics & Multibody Mechanics Research Group (R&MM), Faculty of Mechanical Engineering, Vrije Universiteit Brussel, Belgium. E-mail: tom.verstraten@vub.ac.be

Digital Object Identifier (DOI): see top of this page

II. MODELS

A. Catalog-based motor and gearbox models

1) First Quadrant Constant Efficiency approach (1QCE): In the first approach, we will calculate the energy consumption as if the drive were operated at steady-state conditions in the first quadrant of operation (positive torque and speed). The relation between the torque at the gearbox shaft T_l and the torque at the motor shaft T_m can be calculated if gearbox efficiency η_{tr} and gear ratio n are known:

$$T_l = n\eta_{tr}T_m \tag{1}$$

Assuming that losses do not affect voltage but only current, we can estimate the motor current I based on the motor's torque constant k_t and the catalog efficiency η_m:

$$T_m = k_t\eta_m I \tag{2}$$

The motor's voltage U is a function of the motor's speed constant k_b and motor speed $\dot{\theta}_m = n\dot{\theta}_l$:

$$\begin{aligned} U &= k_b\dot{\theta}_m \\ &= k_b n\dot{\theta}_l \end{aligned} \tag{3}$$

Consequently, the consumed electrical power P_{elec} will be

$$\begin{aligned} P_{elec} &= UI \\ &= \frac{k_b}{k_t\eta_m}\dot{\theta}_m T_m \\ &= \frac{1}{\eta_m\eta_{tr}}\dot{\theta}_l T_l \\ &= \frac{1}{\eta_m\eta_{tr}}P_{mech} \end{aligned} \tag{4}$$

This last formula, which is correct if the motor is constantly operating at its maximum efficiency, is perhaps the most common way of calculating the energy consumed by a motor.

2) Four Quadrant Constant Efficiency approach (4QCE): In four-quadrant operation, power can flow from the motor to the load (quadrants I and III) or vice versa (quadrants II and IV). In the latter case, the load is driving the motor, and the losses must be deducted from the energy of the load instead of the energy at the motor shaft. As proposed in [20], this can be implemented by defining a gearbox efficiency function C_{tr}:

$$C_{tr} = \begin{cases} \eta_{tr} & \text{(load driven by motor)} \\ 1/\eta_{tr} & \text{(motor driven by load)} \end{cases} \tag{5}$$

Equation (1) becomes

$$T_l = C_{tr}nT_m \tag{6}$$

Similarly, we can define a motor efficiency function C_m to rewrite Eq. (2):

$$C_m = \begin{cases} \eta_m & \text{(load driven by motor)} \\ 1/\eta_m & \text{(motor driven by load)} \end{cases} \tag{7}$$

$$T_m = k_t C_m I \tag{8}$$

Motor voltage and electrical power can be calculated by applying equations (3) and (4).

3) Four Quadrant Constant Efficiency approach with motor and gearbox Inertia (4QCEI): The next step is to add the motor and gearbox inertia to the model. If gearbox inertia J_{tr} is specified at the input shaft, the shaft torque becomes

$$T_m = \frac{1}{nC_{tr}}\cdot T_l + J_{tr}\ddot{\theta}_m \tag{9}$$

and a term containing motor inertia J_m is added to Eq. (8):

$$I = \frac{1}{k_t C_m}\left(T_m + J_m\ddot{\theta}_m\right) \tag{10}$$

4) Full DC Motor Model approach (FMM): In this approach, we will use a full DC motor model instead of the motor efficiency function C_m. The equations for motor current (10) and voltage (3) are replaced with

$$\begin{cases} I = \frac{1}{k_t}\left(J_m\ddot{\theta}_m + \nu_m\dot{\theta}_m + T_m\right) \\ U = L\frac{dI}{dt} + RI + k_b\dot{\theta}_m \end{cases} \tag{11}$$

The motor's terminal resistance R_m and inductance L can usually be retrieved from the motor's datasheet. For the motor's viscous damping coefficient ν_m, we will use the estimate

$$\nu_m = \frac{k_t\cdot I_{nl}}{\omega_{nl}} \tag{12}$$

which ensures that, in no-load conditions, a current equal to the no-load current I_{nl} is consumed when the motor is rotating at the no-load speed ω_{nl}.

B. Controller losses

Because we are interested in the total energy consumption of the actuator, experiments will be carried out by measuring the power consumption at the battery terminals. This means that, in addition to the above model, the losses due to the controller need to be calculated. Two types of losses occur:

- *Continuous losses due to controller electronics*: Some manufacturers specify a standby or idle current consumption in their datasheets. This is the current which is continuously drawn from the power source in order to power the electronics. Small, versatile 4-quadrant controllers up to 50W typically consume around 50 mA. By multiplying this current with the power source voltage, the constant power loss $P_{standby}$ due to controller electronics can be calculated. In low-power applications, this loss - typically 1 to 2W - can be a major contributor to the total energy consumption.
- *Losses related to the power flowing through the controller*: In general, datasheets mention a controller efficiency $\eta_{controller}$, typically 90-95%. $\eta_{controller}$ can be used to calculate the power drawn from the power source, P_{source}, by applying following formula:

$$P_{source} = C_c P_{elec} + P_{standby} \tag{13}$$

in which $P_{standby}$ corresponds to the losses due to controller electronics, as explained above, and C_c is the controller efficiency function, defined as

$$C_c = \begin{cases} 1/\eta_{controller} & (P_{elec} > 0) \\ \eta_{controller} & (P_{elec} < 0) \end{cases} \tag{14}$$

In case of the 1QCE model, C_c will be set to $1/\eta_{controller}$ at all time, consistent with the way efficiency is treated in the model.

C. Energy consumption models

1) Integration of power: Following the basic relationship between power and energy, we can calculate the electrical energy consumption E_{elec} from the source power P_{source} by integration of the latter w.r.t. time:

$$E_{elec} = \int P_{source}(t)dt \tag{15}$$

This is the approach which is followed in most branches of physics and engineering, and which should be applied to controllers which allow for regeneration.

2) Integrated absolute power model: In robotics, it is common to make the assumption that the energetic cost of absorbing power is as high as supplying power to the load. Practically, this means that in Eq. (15) the integrand P_{source} should be replaced by its absolute value:

$$E_{elec,abs} = \int |P_{source}(t)|dt \tag{16}$$

Physically, this formula states that, in case of negative power flow, the motor and the controller are receiving energy from both the load and the power source. This would mean that all the energy is dissipated somewhere in these components. While this is rather unlogical, the formula has the benefit of yielding a systematically higher energy consumption than Eq. (15), and can therefore compensate for unmodeled losses, possibly bringing the modeled energy consumption closer to the real energy consumption. As we will demonstrate in Section IV, while in some cases Eq. (16) may lead to results which correspond better to measurements, it is strongly dependent on the model which is used, and can therefore be expected to produce more arbitrary results than Eq. (15).

3) Integrated positive power model: A final approach, which is only followed in a limited number of papers, is the integration of positive power:

$$E_{elec,pos} = \int max\left(0, P_{source}(t)\right) dt \tag{17}$$

This approach would be most suitable if the controller does not allow for regeneration, but braking is possible through the use of braking resistors, or if electronic circuitry is preventing the controller from sending current into the battery. Such protection circuits are common with high-end batteries such as Li-Ion batteries, which may get damaged or even explode if too high reverse currents are applied [21].

Comparing Eq. (17) to Eqs. (15) and (16), one can easily prove that

$$E_{elec,pos} = \frac{1}{2}\left(E_{elec} + E_{elec,abs}\right) \tag{18}$$

In other words, $E_{elec,pos}$ is simply the average of E_{elec} and $E_{elec,abs}$.

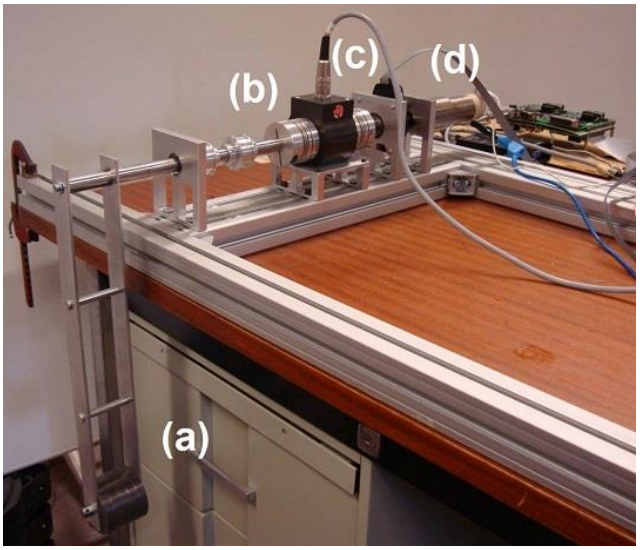

Fig. 1. Pendulum test set-up. Mechanical energy consumption can be calculated from the measurements of the torque sensor (b) and the encoder (c), placed in between the motor-gearbox (d) and the pendulum load (a). Current and voltage are measured at the battery terminals (not shown on picture).

D. Power source losses

The paper only considers the energy consumed at the input of the controller. There is, however, also an efficiency associated with the power source. This is particularly relevant if the power source is a portable unit such as a battery. Lead-acid battery cycle efficiencies are typically around 80 % [22], while the lightweight Li-ion batteries reach efficiencies of around 90% [23]. Additional protection circuits may further decrease these efficiencies. As a consequence of the battery losses, it will not be possible to entirely reuse the energy regenerated by the motor; in other words, the negative power is effectively decreased by the battery efficiency [24]. While a discussion of losses in power sources goes beyond the scope of this paper, readers are encouraged to check for further publications on the energy losses of their specific type of power source, especially if they are considering regeneration as a means to prolong battery life.

III. Test setup

In order to assess the quality of the models established in Section II, they are applied to the setup shown in Fig. 1. The setup consists of a pendulum with properties listed in Table I, driven by a 80 W Maxon DCX35L motor with a planetary gearbox of ratio n=113 (Table II).

The motor will impose a sinusoidal trajectory to the output

$$\theta_l = \theta_0 \sin\left(\omega t\right) \tag{19}$$

TABLE I
Specifications of setup

Mass M	2.493 kg
Moment of inertia in rotation axis J	0.224 kg m^2
Distance from rotation axis to COG l	253.3 mm

TABLE II
SPECIFICATIONS OF GEARBOX AND MOTOR

Nominal power	80 W
Nominal speed	6640 rpm
Nominal torque	120 mNm
No-load speed ω_{nl}	7200 rpm
No-load current I_{nl}	177 mA
Max. motor efficiency η_m	87.8%
Terminal resistance R	0.212 Ohm
Terminal inductance L	0.0774 mH
Torque constant k_t	23.4 mNm/A
Speed constant k_b	408 rpm/V
Rotor inertia J_m	102 gcm^2
Gear ratio n	338/3
Gearbox inertia J_{tr}	5e-7 kg m^2
Gearbox efficiency η_{tr}	72%

with frequencies ω of 0.5, 1, 2 and 5 rad/s and an amplitude θ_0 of 80°. This dynamic task spans all four quadrants of operation and has a net mechanical energy consumption of zero.

The relation between the output angle θ and the gearbox output torque T_l is

$$T_l = J\ddot{\theta} + Mgl\sin(\theta) + sign(\dot{\theta}) \cdot T_C + \nu\dot{\theta} \tag{20}$$

of which the relevant parameters can be found in Table I. Friction is represented by Coulomb friction $sign(\dot{\theta}) \cdot T_C$ and viscous friction $\nu\dot{\theta}$, a generally accepted classic model [25]. The values for T_C and ν were obtained experimentally, and were found to be 0.064 Nm and 0.081 Nms/rad. More elaborate bearing friction models exist which capture temperature and torque-dependent friction, e.g. [26], and include higher-order speed-dependent terms, e.g. [27]. While they may be able to capture more losses and as such significantly improve the quality of the model, the basic friction model employed in Eq. (20) was found adequate for the purpose of comparing the models presented in Section II to the experimental data.

Finally, the mechanical output power can be obtained by multiplying the derivative of Eq. (19) with Eq. (20):

$$P_{mech} = T_l\dot{\theta} \tag{21}$$

The setup allows for a measurement of both mechanical (output) power and electrical (input) power. Mechanical power can be calculated by multiplying the torque, measured by an ETH Messtechnik DRBK-I torque sensor (max. error 0.1Nm), by the speed obtained from a US Digital E6 optical encoder (resolution 2000 counts per turn). Electrical power was calculated as the product of battery voltage and current. The current was measured by an Allegro ACS712 current sensor (max. error 1.5%); the voltage was connected directly to the analog I/O of the National Instruments sbRIO-9626 board used for data acquisition. The sinusoidal trajectory was imposed by a Maxon EPOS2 50/5 motor controller which was powered by two 12V lead-acid batteries placed in series. Every measurement in the following section is the average of at least 10 pendulum periods in order to reduce noise and other non-reproducible effects.

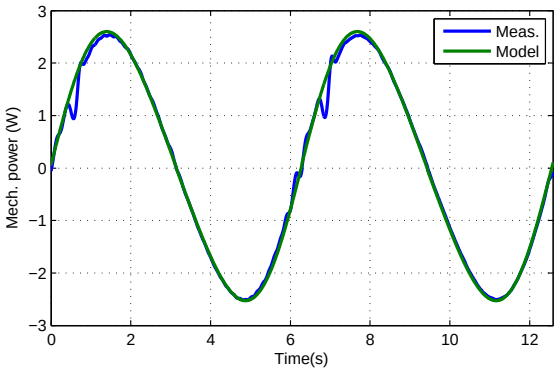

Fig. 2. Measured and modeled mechanical power consumption at the output, for one period of the pendulum at 0.5 rad/s. There is a good match between both, indicating that the mechanical model of the setup is accurate.

IV. RESULTS

A. Mechanical output power

In order to validate the model of the setup, the power profile at the output was measured. The results at 0.5 rad/s are shown in Fig. 2. The good match between the measurement and the model indicate that the parameters of the setup (Table I) are estimated correctly, and that Eq. (20) and Eq. (19) describe the torque and position of the output well. The symmetry of the curve also demonstrates that the amounts of negative and positive work forced upon the load are nearly equal. This symmetry is maintained at higher pendulum speeds.

B. Source power

We will now compare how well the modeled and measured source powers match. Fig. 3 shows the measured and modeled electrical power at the battery terminal, for a pendulum swinging at 0.5 rad/s and 5 rad/s. Note that, unlike the mechanical power, none of the electrical power profiles is symmetrical w.r.t. the power axis. This is mainly caused by the - mostly constant - controller losses, which add an offset to the electrical power curves.

At 5 rad/s, regeneration occurs between 0.1-0.3s and 0.7-0.9s. At 0.5 rad/s however, negative power is completely consumed by the losses, so that none of it is left at the battery terminals. This demonstrates how hard it can be to design a low-power system which can recover energy from the load. To have a considerable amount of negative power available at the load is, obviously, an important condition for energy regeneration, but secondly, the system should also be designed to have a high efficiency, so that this energy is not lost when power is flowing through the actuator. Only if both conditions are met, the negative energy can be used to recharge the battery. A successful example can be found in [28], where the authors performed an experiment in which they managed to regenerate 63% of the negative work.

The discontinuity in the power profiles is not predicted by the 1QCE model because the directionality of gearbox efficiency, which is the cause of this phenomenon, is not incorporated into this model. The results obtained by using

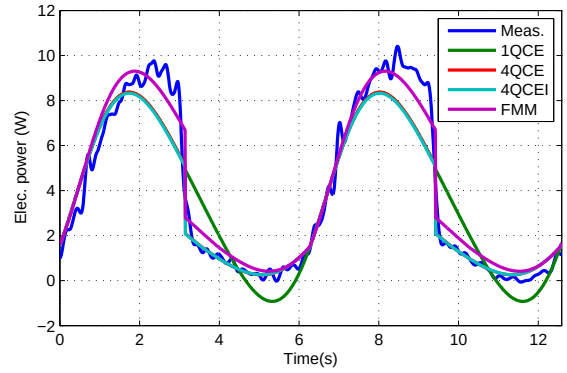

(a) 0.5 rad/s

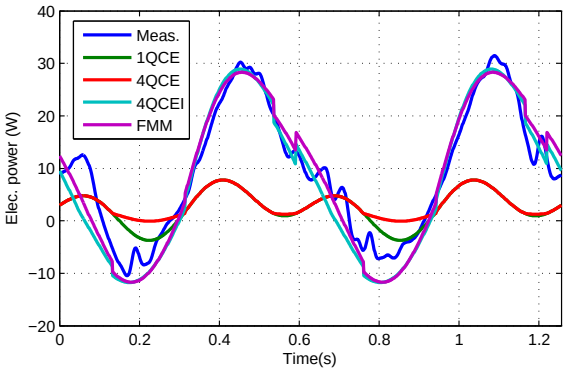

(b) 5 rad/s

Fig. 3. Measured and modeled electrical power consumption at the battery terminals for one period of the pendulum at (a) 0.5 rad/s and (b) 5 rad/s. While the discontinuities in the power profile due to the gearbox efficiency (5) are clearly visible in the measurements at 0.5 rad/s, they are hardly distinguishable in the 5 rad/s measurement. This is due to the time constant of the closed loop system, which is too slow to track the required discontinuous current at this frequency.

this model can therefore be discarded, especially when low-efficiency gearboxes are used. The 4QCE and 4QCEI models yield very similar power profiles at low speed (0.5 rad/s), because the gravitational torque is rather high compared to the inertial torque caused by the motor's acceleration. At higher speeds and accelerations (5 rad/s), however, the power model obtained by the 4QCE model is far from accurate. The peak in electrical power in the 0.5 rad/s measurement occurs at a later time in than predicted by the 4QCE and 4QCEI models, and its amplitude is higher. The FMM model, in which the motor efficiency is load- and speed-dependent, is able to predict this shift, even though it still does not fully match the measurements. A possible cause is the load- and speed dependency of gearbox efficiency, something which is not accounted for in any of the models. Finally, the notches predicted by the FMM and 4QCEI models are not clearly visible in the 5 rad/s power measurement, because the closed loop time constant was too low to track the discontinuity at this speed. Nevertheless, the measurements clearly follow the general trend predicted by the FMM and 4QCEI model. Both models do not differ much in this measurement, because here, the motor operates mostly in regions with near-maximum efficiency. In any case, the measurements indicate that load- and speed-dependent losses affect the input power of an actuated system, and that they can be predicted provided that an adequate model is used.

TABLE III
MEASURED AND MODELED ENERGY CONSUMPTION FOR ONE PENDULUM PERIOD, AT FREQUENCIES OF 0.5, 1, 2 AND 5 RAD/S.

		0.5 rad/s	1 rad/s	2 rad/s	5 rad/s
measured		51.08 J	29.90 J	18.30 J	11.85 J
1QCE	E_{elec}	46.73 J	23.35 J	11.50 J	6.62 J
	$E_{elec,abs}$	49.71 J	36.54 J	29.16 J	7.45 J
4QCE	E_{elec}	45.92 J	27.99 J	17.81 J	7.12 J
	$E_{elec,abs}$	45.92 J	30.67 J	22.76 J	7.13 J
4QCEI	E_{elec}	45.73 J	27.57 J	16.91 J	9.66 J
	$E_{elec,abs}$	45.73 J	29.99 J	20.44 J	16.75 J
FMM	E_{elec}	52.55 J	29.80 J	17.25 J	10.88 J
	$E_{elec,abs}$	52.55 J	31.92 J	20.67 J	17.40 J

C. Consumed energy

Although the comparison of power profiles already gives a lot of information, it is still interesting to see how they translate to energy consumption. The measured and modeled energy consumption of the pendulum at frequencies of 0.5, 1, 2 and 5 rad/s is displayed in Table III. Both equations (15) and (16) are used to derive the energy consumption from the powers obtained by all models presented in Section II-A. The energy consumption derived from Eq. (17), $E_{elec,pos}$, is not included in the table. It was left out because, as explained in Section II-C, it is simply the average of E_{elec} and $E_{elec,abs}$, and therefore does not add anything to the discussion.

Energy consumption decreases with frequency, as the measurements are increasingly nearer to the pendulum's resonance frequency (4.4 rad/s) at which energy consumption is minimal [24], and because the time for the pendulum to complete one period increases as the frequency decreases. The measurements and all models confirm this general trend. The energy consumed by the idle current of the controller is a linear function of time, and so, at low speeds, it will represent a large portion of the energy consumption. At 0.5 rad/s, the idle current causes a loss of 18.6 J (36.4% of the total consumption), whereas at 5 rad/s, this is only 1.9 J (15.7% of total energy consumption). This demonstrates that an energy-efficient controller and, more generally, energy-efficient electronics, can also contribute to the reduction of energy losses, especially in low-power applications.

We will now discuss more specific trends related to the models and the way energy is calculated.

1) E_{elec} vs. $E_{elec,abs}$: Comparing E_{elec} to $E_{elec,abs}$, we observe no difference at all at a frequency of 0.5 rad/s, because the negative power from the load is entirely consumed by the losses. The difference increases at higher frequencies, at which more negative power is available. At 5 rad/s, the E_{elec} value obtained by the FMM model clearly provides the best prediction.

Table III demonstrates a striking trend in the way how modeled energy consumption evolves as the complexity of the model increases. As we move from the simple yet incorrect 1QCE model to the more complex FMM model, which contains more loss mechanisms, we see that, in general, the energy

consumption predicted by E_{elec} is increasing. The inertia of the motor and gearbox may counter this effect (as evidenced by comparing the 4QCE and 4QCEI model at 0.5-2 rad/s) by slightly redistributing the power over the pendulum cycle, but apart from this, there is a clear trend towards increasing energy consumption with increasing model complexity. This is in line with what one would expect: the more losses are considered, the higher the predicted energy consumption will be. Looking at $E_{elec,abs}$, however, there is little consistency in how energy consumption evolves with model complexity. At 5 rad/s, $E_{elec,abs}$ follows the logical trend of increasing energy consumption with increasing model accuracy, whereas at 1 and 2 rad/s, the opposite is true. The least accurate model, the 1QCE model, yields the highest energy consumption $E_{elec,abs}$ at 1 rad/s and 2 rad/s, overestimating the actual consumption by no less than 22.2% and 59.3%. It is the combination of two inaccuracies that causes the predicted energy consumption to boom. First, Eq. (1) will lead to negative power losses in negative power flow, increasing the amount of negative energy instead of reducing it. This conflicts with the "passive sign convention", which states that dissipated power is a positive quantity [29]. Second, this error is amplified by the use of Eq. (16), which converts the - overestimated - negative energy into a positive contribution to the total energy consumption. In conclusion, the results presented in Table III prove that Eq. (16) can lead to serious errors, especially if losses are modeled incorrectly in negative power flow.

2) Comparison between models: The 1QCE model yields very inaccurate energy consumption values, underestimating energy consumption (in case of E_{elec}) by up to 44.1% at 2 rad/s, or overestimating it (in case of $E_{elec,abs}$) by up to 59.3% at 2 rad/s. This comes as no surprise, as in Section IV-B we already pointed out that the measured power profile corresponded very badly with the one obtained from the 1QCE model.

The only difference between the 4QCE and 4QCEI models is the addition of gearbox and motor inertia to the model. Inertia acts as an energy buffer, so intrinsically it does not cause additional energy losses. This is why both models produce very similar energies, especially at low frequencies. One can notice that, moving from the 4QCE to the 4QCEI model, energy consumption decreases at 0.5, 1 and 2 rad/s, but increases at 5 rad/s. By adding gearbox and motor inertia to the model, the total inertia of the modeled system increases, and consequently its resonance frequency ω_0, which is given by

$$\omega_0 = \sqrt{\frac{Mgl}{J + n^2\eta_{tr}(J_m + J_{tr})}} \tag{22}$$

for the linearized system, decreases. With ω_0 = 4.4 rad/s in this particular setup, the 0.5, 1 and 2 rad/s measurements are performed below resonance frequency. In this case, the lowered resonance frequency due to the additional inertias will lead to lower motor currents and powers. The Joule losses being proportional to current squared, this in turn will lead to lower energy losses. Conversely, if a frequency above resonance is imposed, as in the 5 rad/s measurement, the torques and powers will increase, and so will the energy losses in the system.

Finally, there is the FMM model, which incorporates load- and speed-dependent motor losses and is by far the most detailed of the four models. Because the catalog efficiency used in the other models is in fact the maximum efficiency η_m, the energy consumption predicted by the FMM model will always be higher than the 4QCEI model, which assumes a constant motor efficiency of η_m. Looking at E_{elec}, the FMM model produces very decent results, with a maximum error of 8.1% at 5 rad/s. Its underestimation of power consumption indicates that there is still some room for improvement by adding yet unmodeled losses, e.g. speed- and load-dependent gearbox losses, or by improving the current model, e.g. by modeling the influence of motor heating on the motor winding resistance or by increasing the complexity of the friction model, as suggested in Section III.

V. Conclusion

The aim of this paper was to study how well different modeling approaches commonly found in literature can predict the energy consumption of a geared DC motor performing a dynamic task. If one thing stood out clearly from the measurements presented in this paper, it is the importance of defining efficiency functions based on the direction of power flow. If the equations which apply to the 1st quadrant of motor operation are maintained - something which is all too often the case - this can lead to serious errors in the estimated energy consumption. A DC motor model can help to cover more of the load- and speed-dependent losses, and so may a load- and speed-dependent gearbox efficiency model. The latter is more difficult to generate from datasheet information though, and for this reason, it was not studied in this paper. Gearbox and motor inertia have an impact on the resonance frequency of the system, making them particularly relevant for systems which require high accelerations at low torques. While the inertia itself does not cause additional losses, it may cause the total system loss to drop or increase by changing the current flowing through the motor.

Even though the motion demanded equal amounts of positive and negative work to be done on the load, and even though the amount of negative work was substantial, almost none of it was retained at the battery terminals in the slowest measurements. This demonstrates how hard it can be to regenerate negative energy in a simple actuator system. Calculating the energy consumption is by integrating the absolute value of power was shown to be an unreliable method which produces inconsistent results depending on the model which is used to calculate the losses. The physically correct approach of integrating the power itself leads to consistently good results, provided that the system is modeled sufficiently well.

With this paper, the authors hope to have shed some light on the different modeling approaches presented in literature. We hope that the results from this paper will serve as a base from which designers can decide which elements to include in their model, whether their purpose is to compare designs or to get an actual estimate of the consumed power, e.g. for the calculation of power source requirements.

REFERENCES

[1] B. Vanderborght, R. Van Ham, D. Lefeber, T. G. Sugar, and K. W. Hollander, "Comparison of mechanical design and energy consumption of adaptable, passive-compliant actuators," *The International Journal of Robotics Research*, vol. 28, no. 1, pp. 90–103, 2009.

[2] S. Wang, W. van Dijk, and H. van der Kooij, "Spring uses in exoskeleton actuation design," in *Rehabilitation Robotics (ICORR), 2011 IEEE International Conference on*, June 2011, pp. 1–6.

[3] A. Jafari, N. Tsagarakis, I. Sardellitti, and D. Caldwell, "How design can affect the energy required to regulate the stiffness in variable stiffness actuators," in *Robotics and Automation (ICRA), 2012 IEEE International Conference on*, May 2012, pp. 2792–2797.

[4] M. Grimmer, M. Eslamy, S. Gliech, and A. Seyfarth, "A comparison of parallel- and series elastic elements in an actuator for mimicking human ankle joint in walking and running," in *Robotics and Automation (ICRA), 2012 IEEE International Conference on*, May 2012, pp. 2463–2470.

[5] A. Velasco, G. M. Gasparri, M. Garabini, L. Malagia, P. Salaris, and A. Bicchi, "Soft-actuators in cyclic motion: Analytical optimization of stiffness and pre-load," in *IEEE-RAS International Conference on Humanoid Robots*, Atlanta, Georgia, USA, 2013.

[6] N. Paine, S. Oh, and L. Sentis, "Design and control considerations for high-performance series elastic actuators," *Mechatronics, IEEE/ASME Transactions on*, vol. 19, no. 3, pp. 1080–1091, June 2014.

[7] P. Beckerle, J. Wojtusch, S. Rinderknecht, and O. von Stryk, "Analysis of system dynamic influences in robotic actuators with variable stiffness," *Smart Structures and Systems*, vol. 13, no. 4, pp. 711–730, 2014.

[8] W. Brown and A. Ulsoy, "A passive-assist design approach for improved reliability and efficiency of robot arms," in *Robotics and Automation (ICRA), 2011 IEEE International Conference on*, May 2011, pp. 4927–4934.

[9] S. Au and H. Herr, "Powered ankle-foot prosthesis," *Robotics Automation Magazine, IEEE*, vol. 15, no. 3, pp. 52–59, September 2008.

[10] M. Plooij and M. Wisse, "A novel spring mechanism to reduce energy consumption of robotic arms," in *Intelligent Robots and Systems (IROS), 2012 IEEE/RSJ International Conference on*, Oct 2012, pp. 2901–2908.

[11] E. Rouse, L. Mooney, E. Martinez-Villalpando, and H. Herr, "Clutchable series-elastic actuator: Design of a robotic knee prosthesis for minimum energy consumption," in *Rehabilitation Robotics (ICORR), 2013 IEEE International Conference on*, June 2013, pp. 1–6.

[12] M. A. Holgate, J. K. Hitt, R. D. Bellman, T. G. Sugar, and K. W. Hollander, "The SPARKy (Spring Ankle with Regenerative Kinetics) project: Choosing a DC motor based actuation method," in *2nd IEEE/RAS-EMBS International Conference on Biomedical Robotics and Biomechatronics*. IEEE, 2008, pp. 163–168.

[13] C. Everarts, B. Dehez, and R. Ronsse, "Variable stiffness actuator applied to an active ankle prosthesis: Principle, energy-efficiency, and control," in *Intelligent Robots and Systems (IROS), 2012 IEEE/RSJ International Conference on*, Oct 2012, pp. 323–328.

[14] M. Zinn, B. Roth, O. Khatib, and J. K. Salisbury, "A new actuation approach for human friendly robot design," *The International Journal of Robotics Research*, vol. 23, no. 4-5, pp. 379–398, 2004.

[15] J. Schuy, P. Beckerle, J. Faber, J. Wojtusch, S. Rinderknecht, and O. Stryk, "Dimensioning and evaluation of the elastic element in a variable torsion stiffness actuator," in *Advanced Intelligent Mechatronics (AIM), 2013 IEEE/ASME International Conference on*, July 2013, pp. 1786–1791.

[16] Q. Cao and I. Poulakakis, "On the energetics of quadrupedal bounding with and without torso compliance," in *Intelligent Robots and Systems (IROS 2014), 2014 IEEE/RSJ International Conference on*, Sept 2014, pp. 4901–4906.

[17] M. Laffranchi, L. Chen, N. Tsagarakis, and D. Caldwell, "The role of physical damping in compliant actuation systems," in *Intelligent Robots and Systems (IROS), 2012 IEEE/RSJ International Conference on*, Oct 2012, pp. 3079–3085.

[18] F. Roos, H. Johansson, and J. Wikander, "Optimal selection of motor and gearhead in mechatronic applications," *Mechatronics*, vol. 16, no. 1, pp. 63 – 72, 2006.

[19] A. Werner, R. Lampariello, and C. Ott, "Optimization-based generation and experimental validation of optimal walking trajectories for biped robots," in *Intelligent Robots and Systems (IROS), 2012 IEEE/RSJ International Conference on*. IEEE, 2012, pp. 4373–4379.

[20] H. Giberti, S. Cinquemani, and G. Legnani, "Effects of transmission mechanical characteristics on the choice of a motor-reducer," *Mechatronics*, vol. 20, no. 5, pp. 604 – 610, 2010.

[21] D. Andrea, *Battery Management Systems for Large Lithium Ion Battery Packs*. Artech House, 2010.

[22] J. Stevens and G. Corey, "A study of lead-acid battery efficiency near top-of-charge and the impact on pv system design," in *Photovoltaic Specialists Conference, 1996, Conference Record of the Twenty Fifth IEEE*, May 1996, pp. 1485–1488.

[23] C. J. Rydh and B. A. Sandén, "Energy analysis of batteries in photovoltaic systems. part I: Performance and energy requirements," *Energy Conversion and Management*, vol. 46, no. 1112, pp. 1957 – 1979, 2005.

[24] T. Verstraten, G. Mathijssen, R. Furnémont, B. Vanderborght, and D. Lefeber, "Modeling and design of geared DC motors for energy efficiency: Comparison between theory and experiments," *Mechatronics*, vol. 30, pp. 198 – 213, 2015.

[25] H. Olsson, K. Åström, C. C. de Wit, M. Gäfvert, and P. Lischinsky, "Friction models and friction compensation," *European Journal of Control*, vol. 4, no. 3, pp. 176 – 195, 1998.

[26] A. Bittencourt, E. Wernholt, S. Sander-Tavallaey, and T. Brogardh, "An extended friction model to capture load and temperature effects in robot joints," in *Intelligent Robots and Systems (IROS), 2010 IEEE/RSJ International Conference on*, Oct 2010, pp. 6161–6167.

[27] L. Simoni, M. Beschi, G. Legnani, and A. Visioli, "Friction modeling with temperature effects for industrial robot manipulators," in *Intelligent Robots and Systems (IROS), 2015 IEEE/RSJ International Conference on*, 2015.

[28] S. Seok, A. Wang, M. Y. Chuah, D. Otten, J. Lang, and S. Kim, "Design principles for highly efficient quadrupeds and implementation on the MIT Cheetah robot," in *Robotics and Automation (ICRA), 2013 IEEE International Conference on*, May 2013, pp. 3307–3312.

[29] D. Y. Goswami, *The CRC handbook of mechanical engineering*. CRC press, 2014.